

Article

Not peer-reviewed version

Excitation Pulse Influence on the Accuracy and Robustness of Equivalent Circuit Model Parameter Identification for Li-Ion Batteries

[Dmitrii Grebtsov](#) , [Alexey Druzhinin](#) , [Artem Sergeev](#) *

Posted Date: 15 December 2025

doi: 10.20944/preprints202512.1303.v1

Keywords: equivalent circuit model; Li-ion battery; battery management system; parameters estimation



Preprints.org is a free multidisciplinary platform providing preprint service that is dedicated to making early versions of research outputs permanently available and citable. Preprints posted at Preprints.org appear in Web of Science, Crossref, Google Scholar, Scilit, Europe PMC.

Copyright: This open access article is published under a [Creative Commons CC BY 4.0 license](#), which permit the free download, distribution, and reuse, provided that the author and preprint are cited in any reuse.

Disclaimer/Publisher's Note: The statements, opinions, and data contained in all publications are solely those of the individual author(s) and contributor(s) and not of MDPI and/or the editor(s). MDPI and/or the editor(s) disclaim responsibility for any injury to people or property resulting from any ideas, methods, instructions, or products referred to in the content.

Article

Excitation Pulse Influence on the Accuracy and Robustness of Equivalent Circuit Model Parameter Identification for Li-Ion Batteries

Dmitrii Grebtsov ¹, Alexey Druzhinin ¹ and Artem Sergeev ^{1,2,*}

¹ Moscow Center for Advanced Studies, Moscow 123592, Russia

² N.N. Semenov Federal Research Center for Chemical Physics, Moscow 119991, Russia

* Correspondence: a.sergeev@chph.ras.ru

Abstract

An equivalent circuit model (ECM) is a highly practical tool for simulating Li-ion battery behavior. There are many relevant studies which compare different ECM variants or suggest algorithms to extract model parameters from the experimental data. However little attention has been given to the battery tests used for identification of the ECM parameters. Therefore, we systematically studied the influence of experimental test pulse characteristics on the parameterized ECM accuracy. Test pulse duration and amplitude were varied along with the portion of the relaxation phase data used by the parameters fitting algorithm. That resulted in 168 parameter sets, each validated using 9 diverse current profiles including one based on a realistic drive cycle. The validation results prove that the impact of the test pulse choice on the parameterized ECM accuracy is great to the point it can overshadow the use of a higher order Thevenin model. By choosing the optimal parameter set the simulated voltage root mean square error was reduced to as low as 1.2 mV.

Keywords: equivalent circuit model; Li-ion battery; battery management system; parameters estimation

1. Introduction

Accurate estimation of state of charge (SoC) and state of health (SoH) is crucial for the efficient and safe operation of lithium-ion (Li-ion) batteries in applications such as electric vehicles, portable electronics, aviation, and stationary energy storage systems [1]. Battery Management Systems (BMS) rely on mathematical models to estimate the battery state. An accurate digital Li-ion cell model is also a useful tool for battery pack design and engineering as it can significantly accelerate the design process by enabling virtual experiments and testing. The choice of the most suitable model faces a fundamental trade-off between the model accuracy and its complexity and computational burden, as many applications imply real-time simulations relying on limited on-board computational resources. From a practical perspective, there is another factor – how difficult it is to identify all the required model parameters.

There are three main types of Li-ion battery models: electrochemical models, equivalent circuit models, and data-driven models. The electrochemical models implement an ab initio approach by explicitly taking into account physicochemical processes taking place within an electrochemical cell operation (ions diffusion, charge transfer, reaction kinetics) [2,3]. Such models enable deep analysis of the design-performance relationships and therefore are useful for research and development at the cell level. However, the computational complexity of such models makes them hardly applicable for BMS use and battery pack engineering (since it involves simulations of dozens and hundreds of cells) [4].

Equivalent circuit models (ECM) and data-driven models both use an empirical approach, aiming to predict battery behavior without explicitly modeling the internal processes. The relatively

new and promising data-driven models are based on machine learning methods and, potentially, are able to capture complex non-linear dependencies between the input and output signals of the system [5,6]. However, the data-driven models are quite complex to tune and run, usually require an extensive training data set, and may fail badly outside the conditions phase space covered by the training set. Therefore, relatively simple ECMs are the most widely used in BMS and battery design applications.

An ECM describes the Li-ion cell as an electric circuit consisting of few components. A Thevenin model is one of the most commonly used ECMs. It consists of a voltage source (open-circuit voltage, OCV), a series ohmic resistance (R_0), and a number of resistance-capacitor (RC) pairs that model dynamic polarization [1,7] (see Figure 1). The order of the ECM defines the number of the included RC-circuits. A relatively simple model design provides several advantages: ease of implementation, low computational load and physical intuitiveness. The latter means that the parameters of the circuit components can be correlated to the physical parameters of a real electrochemical cell (e.g., electrode surface resistance and ion diffusion coefficients).

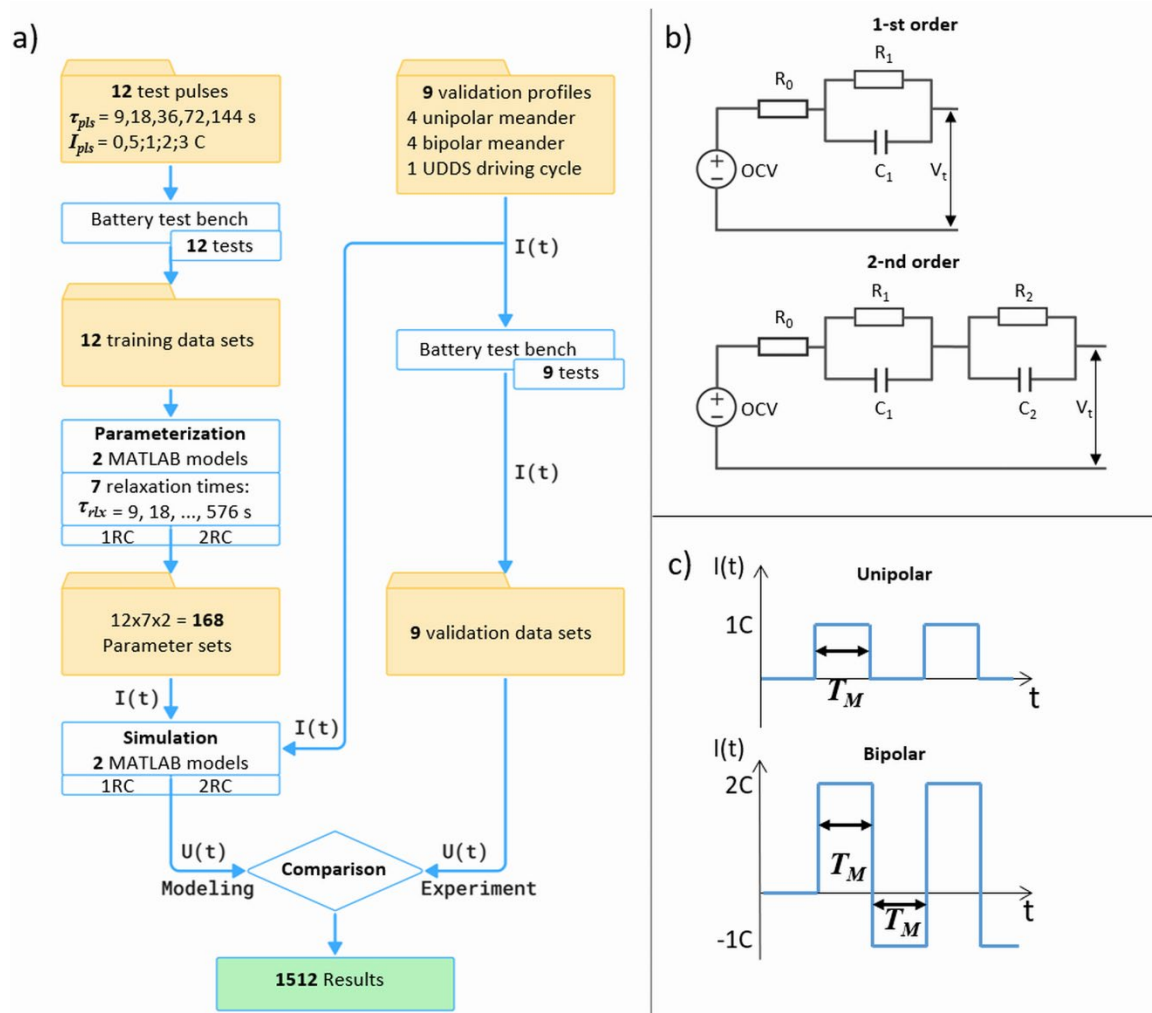


Figure 1. (a) A schematic illustration of the workflow; (b) the considered equivalent circuit models; (c) two shapes of the meander-like validation profiles.

Cell voltage relaxation in response to a sudden current change results from multiple dynamic processes with different time scales, such as electric double layer charging, electrolyte diffusion, and solid-phase diffusion [8]. A 1st-order ECM effectively captures the main dynamic characteristics of the battery response requiring minimal computational efforts, while only one time-constant identification is required. This model is widely used in industrial applications due to its reliability

and ease of parameterization [9]. However, it is inherently unable to provide high accuracy. A second-order Thevenin model enables a more accurate approximation of the cell voltage dynamics by separating fast (high-frequency) and slow (low-frequency) transient processes. The first RC circuit is often associated with the electric double layer charging process, and the second one — with the solid-phase diffusion [8,10,11]. Therefore, the second-order models are assumed to be significantly more accurate than the first-order models while maintaining acceptable computational complexity.

Higher-order ECMs (3rd and above) can hypothetically provide even higher accuracy. However, a comparison study has shown that the 2nd-order ECM yields the lowest error [7]. The possible reason is that the identification of the additional parameters describing the extra RC pairs makes the results unstable because of the risk of overfitting and difficulties in separating processes with similar time constants. A critical problem highlighted in [12] is the ambiguity in parameter identification: the same voltage transient response can be approximated with equal accuracy by several different sets of ECM parameters. That makes the results of high-order ECM parameterization highly dependent on the chosen algorithm and initial approximations, and consequently, unpredictable and poorly interpretable. Thus, the high-order ECMs are impractical for most applications.

The accuracy of any ECM model critically depends on the correct identification of its parameters (R_0 , R_1 , C_1 , R_2 , C_2), which, in turn, non-linearly depend on the cell state of charge, operation temperature, and state of health [10,13]. The most common and practical approach to ECM parameterization is based on the analysis of the voltage response to rectangular current pulses, for example, tests using the Hybrid Pulse Power Characterization (HPPC) technique [14]. There are different ways to extract the model parameters from the cell voltage response to the test pulse. Some authors employ simple analytical equations [10], while most researchers employ fitting procedures based on least squares algorithms that iteratively adjust the parameters to minimize the difference between the measured voltage and the model prediction. A lot of efforts were made in order to develop advanced parameters identification algorithms. Specifically, researchers had suggested several methods to separate the fast and slow dynamics contributions [12,15,16].

Although first and second order ECMs are widely used and there are many studies focused on parameter identification algorithms, the literature still lacks a systematic investigation of how the characteristics of the test pulse (i.e., amplitude and duration) affect the reliability of the parameterization process and, consequently, the accuracy of the model. Numerous studies employing pulse excitation techniques (such as HPPC, GITT, DST) for the model parameterization groundlessly select the durations of the test pulse and the following relaxation phase. There is a wide scatter of the test pulse duration values: 10 s [17–19], 18 s [20], 20 s [21], 30 s [22], 45 s [12], 60 s [22], 90 s [12,23], 180 s [12,23,24], 360 s [12,23,25], 720 s [26] and 900 s [27]. The length of the post-pulse relaxation segment processed by the parameter identification algorithm is also scattered widely or is not even stated clearly in many sources. Few studies have taken effort to compare different test pulses. However, they are limited to a very small number of combinations of test conditions (e.g., four [28] and five [23]).

The goal of the current study is to systematically investigate the impact of the test pulse characteristics and the length of the processed relaxation data segment on the accuracy of the Thevenin model conditioned by the identified set of parameters. The general workflow is illustrated in Figure 1a. The ECM parametrization was performed using 12 experimental data sets based on test pulses characterized by different combinations of pulse duration τ_{pls} and pulse current I_{pls} . Two models were parametrized for each data set: 1RC and 2RC (see Figure 1b). For a specific test pulse and a selected model, 7 parameter sets were obtained by varying the length of the relaxation data segment (τ_{rlx}) processed by the parameter fitting algorithm. That yielded $12 \times 2 \times 7 = 168$ parameter sets. In contrast to the available literature data the extended number of parametrization condition combinations enabled us to perform a systematic search for the optimal one. The accuracy of the models was estimated for each parameter set using 9 different validation profiles, so that the final analysis is based on a total of 1512 individual results. It was found that the optimal test pulse characteristics depend on the cell operation regime. Nevertheless, some general trends were deduced

which favor a longer test pulse duration. By simultaneously tuning the test pulse and relaxation data segment length we were able to reach an excellent accuracy of both the 1st and 2nd order ECMs when validated against a realistic current profile typical for the electric vehicle application.

2. Methods

2.1. Measurements Setup and Procedure

The experimental measurements were performed using a Neware CT-4008Tn-5V12A-S1 test station on a 3500 mAh LG INR18650 MJ1 Li-ion cell. The procedure started with an initial capacity verification cycle to precisely determine the reference capacity. Subsequently, the open circuit voltage (OCV) versus state of charge (SoC) relationship was characterized using two methods: a low-rate (C/20) full cycle and an incremental step discharge test (5% SoC steps) with prolonged relaxation periods to record the equilibrium voltage at each point. According to the low-rate discharge measurements, the cell capacity is 3.36 ± 0.01 Ah, therefore, later on the current value of 1C is equal to 3.36 A.

Following the OCV-SoC calibration, dynamic pulse tests were performed within a mid-range SoC window (55-45%) to generate data for parameterization of battery models. Finally, to validate the models under realistic conditions, variational tests were performed according to 9 different current profiles. All experiments were carried out in a controlled temperature environment of 27 ± 3 °C.

2.2. Parametrization Procedure

Based on the literature data, two equivalent circuit models were selected for the study, which are first-order ('1RC') and second-order ('2RC') Thevenin models, as depicted in Figure 1b. Beside OCV-SoC dependence, these models require the identification of 3 and 5 SoC-dependent parameters, respectively. Namely: serial resistance R_0 , polarization resistances R_1 and R_2 , RC-circuit time constants τ_1 , τ_2 . In all cases, these parameters were identified by processing the cell voltage response to the test pulses. The identification was performed for three SoC values: 55%, 50% and 45%. It is well known that the Li-ion battery OCV demonstrates most rapid changes near the fully charged and discharged states. Therefore, model parametrization within high and low SoC ranges requires more SoC points. However, in real-life scenario batteries operates in the middle SoC range most of the time. Thus, we focused on the middle SoC range in order to reduce the number of experiments and avoid sharp parameter changes typical for high and low SoC while investigating the fundamental trends. A table-based Thevenin Li-ion cell model implemented in the MATLAB Simscape software package was used to simulate cell operation. A set of MATLAB scripts were developed by the authors to perform model parameters fitting and model validation. The parameter identification was carried out by minimizing the cell voltage root mean square error (RMSE) using a non-linear least squares algorithm.

The experimental data segment used for parameter identification consisted of a current test pulse (duration τ_{pls}) and the initial segment (duration τ_{rlx}) of the following relaxation period, so the total duration of the processed experimental data segment was $\tau_{pls} + \tau_{rlx}$. It should be noted, that the overall relaxation period length was 3 hours in order to ensure that the cell had reached the equilibrium state before exerting the next test pulse. However, the relaxation data were cut to τ_{rlx} before the parameter identification. This limitation was imposed as even small voltage error at an hour-timescale can overshadow the contribution of the transient processes of interest to the total RMSE value, which is the target value of the minimization algorithm. The impact of the relaxation data cutoff on the parameterization results was studied by varying τ_{rlx} in the range 9, 18, 36, 72, 144, 288 and 576 s.

2.3. Test Pulse Set

In the current study, two parameters of a test pulse were varied: test pulse duration τ_{pls} and test pulse current amplitude I_{pls} . The complete set of the total of 12 combinations considered is presented

in Table 1. The current amplitudes are expressed in C-rates, where 1C corresponds to 3.36 A according to the measured cell capacity. The widely used approach to the battery ECM parameterization implies that the parameters are identified locally with respect to the SoC. Therefore, the test pulse duration and current are limited by the requirement for a small SoC change. The combinations [144 s / 0.5C] and [72 s / 1C] yield a change in SoC 2% that was considered a reasonable upper limit.

Table 1. The set of test pulses adopted in this study characterized by the pulse duration and amplitude.

Test pulse duration, τ_{pls}	0.5C	1C	2C	3C
9 s	+	+	+	+
18 s	+	+	+	
36 s	+	+		
72 s	+	+		
144 s	+			

2.4. Validation Profiles

For validation of the obtained ECM parameter sets, we used a total of 9 validation current profiles including 8 meander-like profiles and one profile based on the Urban Dynamometer Driving Schedule (UDDS) driving cycle [29]. The shapes of the meander-like validation profiles are presented in Figure 1c. The meander period (T_M) was set to 3, 10, 30 and 180 seconds in order to represent battery operation modes characterized by different power consumption time scale. These profiles are labeled below as 'M03', 'M10', 'M30' and 'M180' respectively. The mean current value was equal to 0.5C, so that the average discharge rates are the same for all meander-like validation profiles. However, 4 profiles are unipolar, i.e., include only negative (discharge) current pulses and rest periods, while the other 4 profiles are bipolar, i.e., consist of alternating negative and positive (charge) current pulses. The bipolar profiles represent energy recuperation typical for electric vehicle applications and energy buffering operation mode typical for the grid applications. The ninth UDDS-based validation profile models the electric vehicle battery current demand profile. In contrast to the meander-like profiles, it has irregular shape close to the real-world scenario. It should be noted that the average discharge rate of the UDDS profile is 0.1C. Therefore, the model error values yielded by the UDDS profile validation should not be compared directly to the error values yielded by the meander profiles validation.

2.5. Udds Profile Adaptation

To convert the Urban Dynamometer Driving Schedule (UDDS) speed profile into a battery current profile, a model of an electric vehicle powertrain described in works [30,31] was implemented using AMESim software. This approach takes into account the vehicle's dynamic characteristics, including various resistive forces: aerodynamic drag, rolling resistance, inertia force, and gravitational component on slopes. The UDDS speed profile (Figure 2a) [29] served as an input signal for the electric vehicle model. The power required to maintain the specified speed at the wheels was calculated by the mechanical part of the model and passed to the power conversion part of the model (electric motor, inverter, etc.), which yielded battery power consumption P_{batt} . The battery current was calculated as $I_{batt} = P_{batt}/U_{batt}$, where U_{batt} is the battery voltage. The U_{batt} was set as a constant to simplify the calculations at this stage (nominal cell voltage 3.63 V). For the main ECM simulations, the current profile was used instead of the power profile because the cyclor controller software worked directly with the current values. The current values were scaled to a single cell.

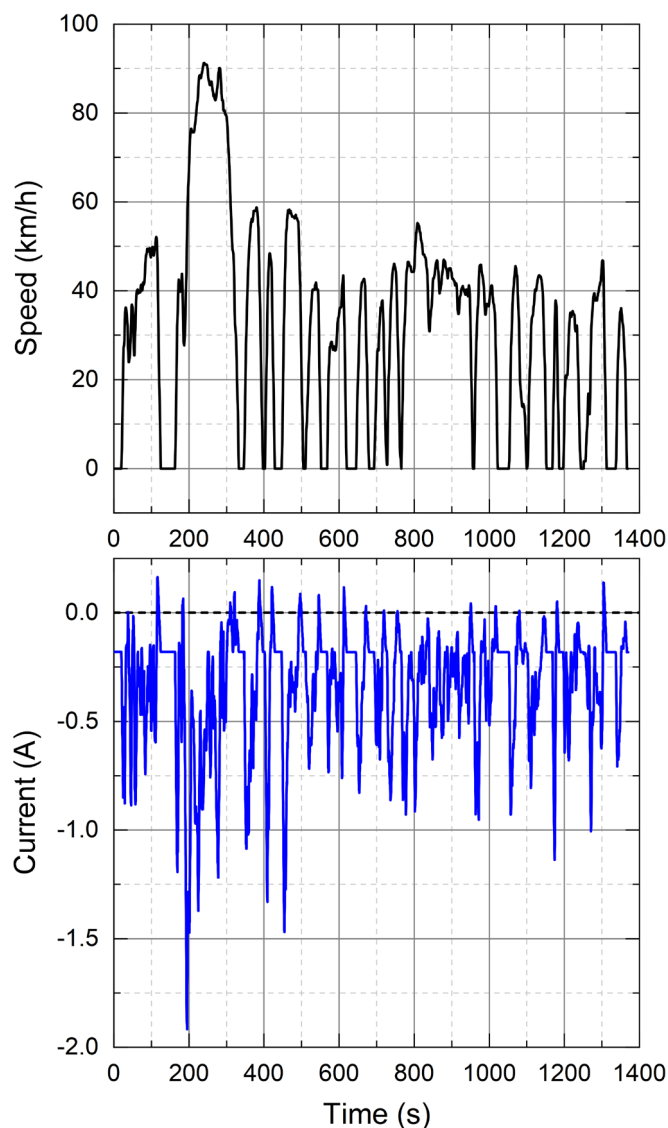


Figure 2. (a) UDDS driving cycle velocity profile; (b) the calculated battery current profile used for ECM validation.

The obtained current profile (Figure 2b) preserves all characteristic features of the original UDDS driving cycle: acceleration phases, steady driving, braking, and recuperation (charging current). This ensures an adequate assessment of the ECM performance under conditions close to real electric vehicle operation.

3. Results and Discussion

We begin by assessing the impact of the order of the Thevenin model. As was discussed in the Introduction section, most of the literature sources agree that the second-order ECM is an optimal choice, which provides reasonable accuracy while avoiding high computational costs and problems associated with simultaneous identification of a large number of model parameters. However, direct comparison of models is tricky, because the ECM accuracy heavily depends on the quality of the parameter set used, while different order models require different parameter sets. Therefore, Figure 3-ino shows the RMSE values for the 1RC and 2RC models averaged over all parameter sets obtained for different τ_{pls} , I_{pls} , τ_{rlx} . The 2RC model does yield a smaller average error for every validation case. However, the difference is not crucial. The average relative reduction in the RMSE values ranges from 10% (UDDS) to 26% (M03 bipolar validation profile).

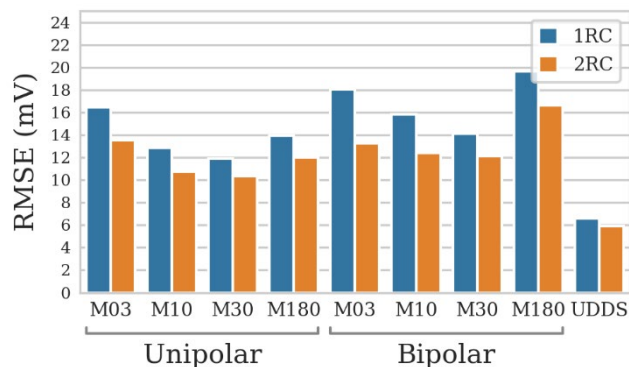


Figure 3. The RMSE values calculated for different validation profiles and averaged over all the obtained parameter sets.

Moreover, the 1RC model based on the optimal parameter set can be more accurate than the 2RC model based on an arbitrary chosen parametrization protocol. For example, Figure 4 shows the spread of the RMSE values for some validation cases. The semitransparent areas depict the error range across the considered relaxation data cutoff values τ_{rlx} , the lower edge reflects the best accuracy, the points reflect the average value (calculated across different τ_{rlx} under fixed τ_{pls} value). Although the minimum possible RMSE value is obtained using the second-order model, the areas associated with the 1RC and 2RC models overlap significantly. The same is true for all the other validation cases. Thus, the higher ECM order per se does not guarantee the accuracy superior to the lower order models if the parameterization procedure was not chosen carefully.

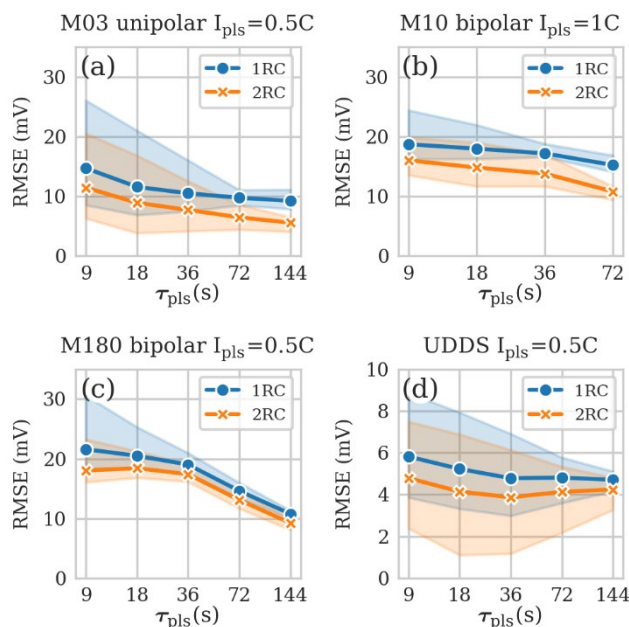


Figure 4. The dependences of the RMSE on the test pulse duration τ_{pls} compared for the 1RC and 2RC models. The RMSE value spread across the relaxation segment lengths τ_{rlx} is depicted by the semitransparent areas, the marked lines represent the values averaged over τ_{rlx} . The test pulse amplitude values and the validation profile names are noted above the graphs.

It should be noted, that regardless of the number of RC-circuits ECM remains a linear system with respect to current-voltage response, while a real battery is only close to linearity to some extent. Therefore, the amplitude of the exciting current pulse may affect the values of the identified model

parameters. Figure 5 illustrates the dependence of the model error on the amplitude of the test pulse used for the model parameterization. Two types of error values are shown: the minimum RMSE value across the parameter sets with different τ_{rlx} and the mean value across the same sets. In most of the cases, the 0.5C test pulses yield noticeably more accurate parameter sets than the higher amplitude test pulses (M180 bipolar being the only exception). This result is quite interesting, as the amplitudes of the meander-like current profiles used for the validation were 1C and 2C for the unipolar and bipolar profiles, respectively. The Thevenin model is inherently unable to reproduce the non-linear effects, but in order to correctly capture the linear portion of the battery response one should set moderate amplitude of the test pulses. (However, the voltage response must be much greater than the instrumental noise, therefore, we discourage the use of test pulses extremely low-amplitude test pulses.) In the following, our analysis will be limited to parameter sets based only on 0.5C test pulses ($I_{\text{pls}} \approx 0.5\text{C}$).

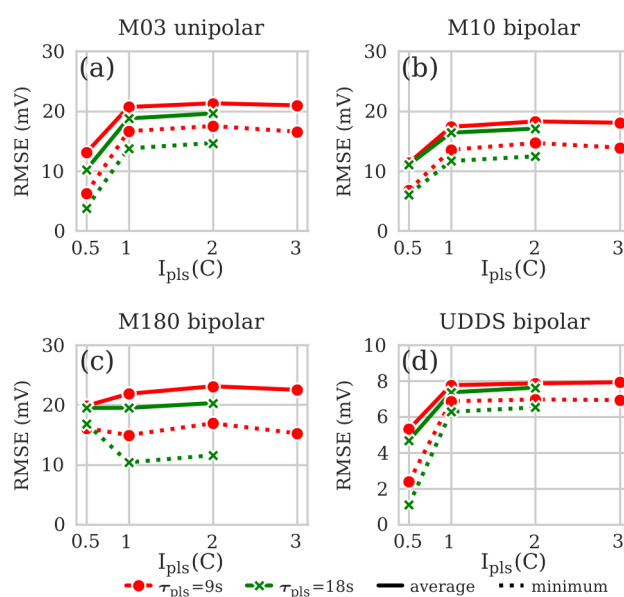


Figure 5. The dependences of the RMSE on the test pulse amplitude I_{pls} for the 2 RC model. The solid lines represent the RMSE value averaged over the relaxation segment lengths τ_{rlx} , while the dashed lines represent the best result. The validation profile names are noted above the graphs.

Although the Thevenin models usually contain more than one RC-circuit to describe several transient processes with different characteristic times, it is implied that the excitation and relaxation phases of those processes are symmetric with respect to time as the capacitors charging and discharging rates are governed by the same time constant. Battery voltage polarization is the result of several complex physical processes, including lithium intercalation and diffusion within the electrode material. Taking into account that the reaction rate constants and solid-phase diffusion coefficients depend on local lithium concentration [32], there is no guarantee that the characteristic times of the excitation and relaxation phases are exactly the same.

Some researchers suggest to identify the ECM parameters solely on the basis of either the cell voltage dynamics during the excitation phase [10] or the voltage relaxation following the current pulse [23], while others utilize both the pulse and the relaxation data segments [12]. In the current study, we vary the impact of the excitation and relaxation phases on the values of the identified parameters by choosing different combinations of τ_{pls} , and τ_{rlx} . The calculated RMSE values for the parameter sets obtained using 0.5C current pulses are presented in Figure 6 as a set of heatmaps. Each heatmap covers all combinations of test pulse durations τ_{pls} and relaxation data cutoff values τ_{rlx} validated using one of the nine current profiles.

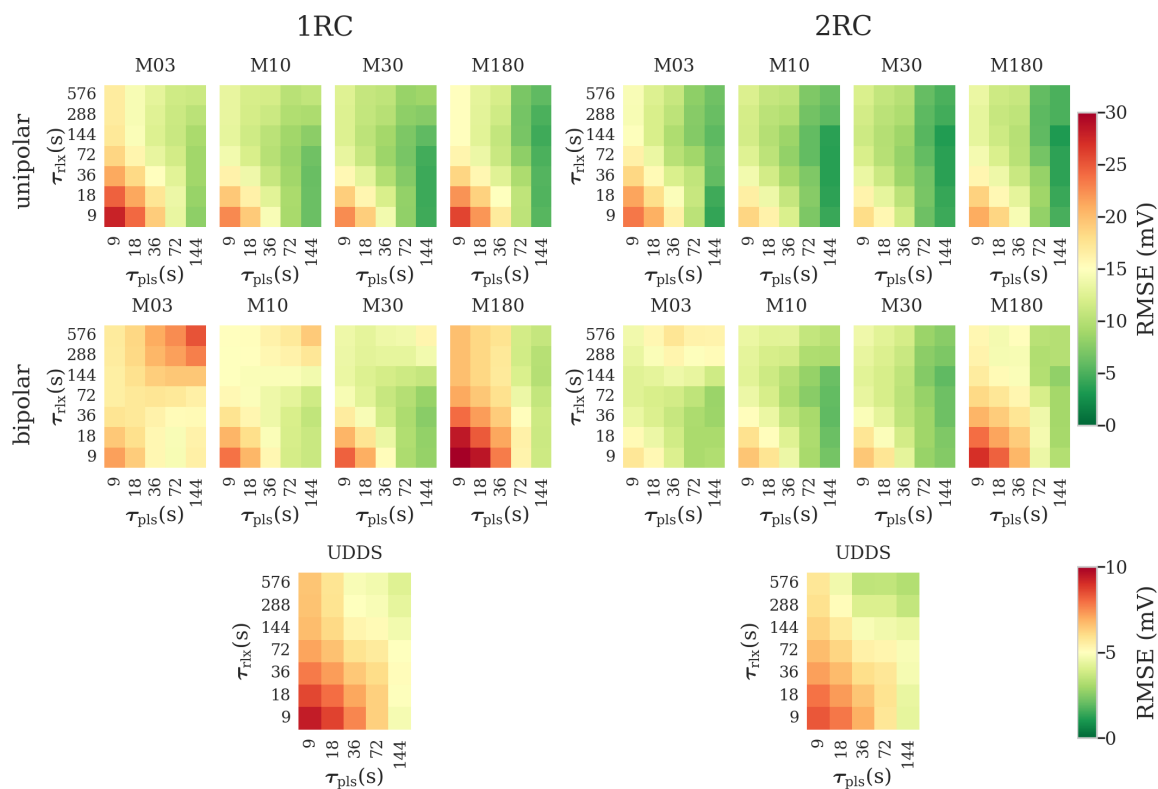


Figure 6. A set of heatmaps visualizing the RMSE of the models based on different parameter sets. The test pulse amplitude is $I_{pls} = 0.5$ C. Note that the UDDS validation heatmaps have a separate color scale.

The shortest pulse duration ($\tau_{pls} = 9$ s) supplemented by the shortest relaxation segment ($\tau_{rix} = 9$ s) results in a large error value in all validation cases. However, it is hard to deduce a universal recommendation for choosing the optimal parameter set. The heatmaps in Figure 6 show that the trends with respect to varying τ_{pls} , and τ_{rix} depend on the validation profile used to estimate the error. Therefore, the optimal model parameterization protocol would depend on the presumptive battery operation regime.

Generally, increasing the duration of the test pulse helps to improve the accuracy. For many validation profiles, the best parameter sets are obtained using the longest $\tau_{pls} = 144$ s. This value is very different from the test pulse duration of about 10 – 30 s commonly used for ECM parameterization according to the literature. The long test pulse duration is especially beneficial for the M30 and M180 validation profiles. Thus, if the battery operation regime implies a constant, slowly changing, or infrequently changing current profile, the test pulse duration should be set to about 2 minutes or longer. With respect to the relaxation data cut-off, the optimal τ_{rix} is within the range of 36 to 144 s for most of the meander-like profiles. Higher τ_{rix} values decrease the accuracy of the model.

In case of UDDS validation profiles, the optimal conditions are shifted to a shorter τ_{pls} (18 - 36 s) and longer relaxation segment length $\tau_{rix} = 576$. In order to verify that the $\tau_{rix} = 576$ yields the best possible results, additional parameter sets were generated using even larger relaxation cut-off times: 1152 and 2304 seconds. These parameter sets indeed turned out to be slightly less accurate. Thus, both in the case of meander-like and UDDS validation profiles, there is a certain limit to which increasing the relaxation data segment can improve the model accuracy.

Finally, Figure 7 demonstrates the accuracy of the first- and second-order models that rely on the best set of parameters ($\tau_{pls} = 36$ s, $\tau_{rix} = 576$ s, $I_{pls} = 0.5$ C) obtained for the UDDS validation profile. 1RC: RMSE – 3.0 mV, maximum absolute error – 7.3 mV; 2RC: RMSE – 1.2 mV, maximum absolute error – 5.6 mV. Note that the RMSE values averaged over all the parameter sets obtained are 6.8 mV (1RC) and 6.5~mV (2RC), so that the errors were reduced by 56% and 82%, respectively. Taking into

account that a typical OCV slope of an NMC battery within the mid-SoC region is about 8-10 mV per 1% SoC, the parameterized model can be used to trace the battery SoC with excellent precision.

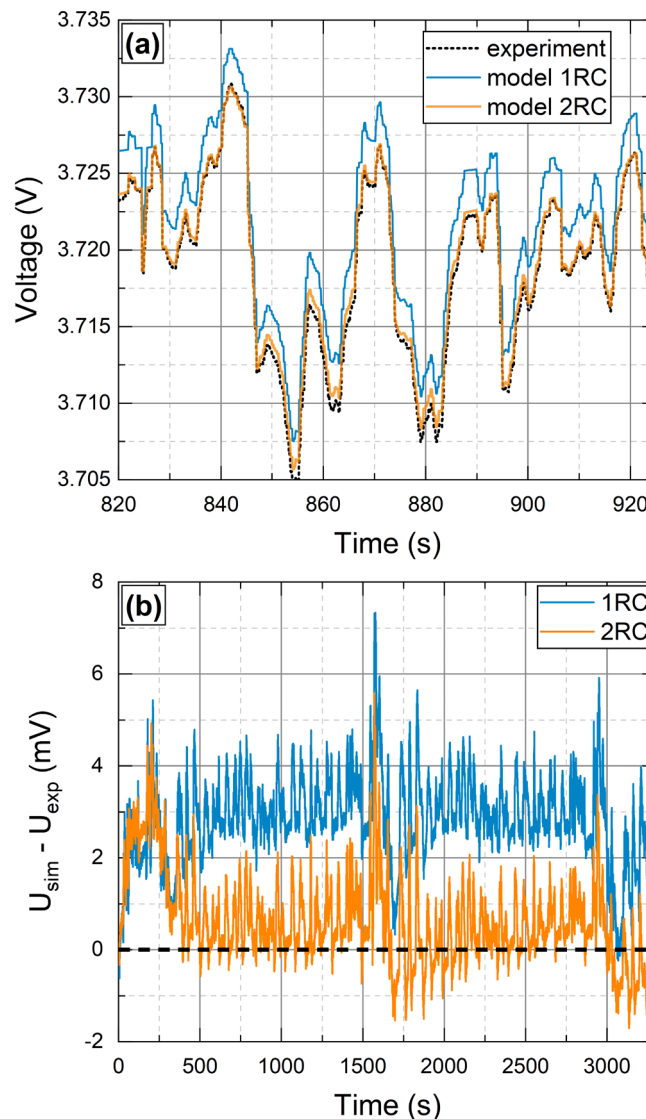


Figure 7. A set of heatmaps visualizing the RMSE of the models based on different parameter sets. The test pulse amplitude is $I_{\text{pls}} = 0.5$ C. Note that the UDDS validation heatmaps have a separate color scale.

5. Conclusions

This systematic study demonstrates that the test pulse duration, amplitude, and relaxation data cutoff significantly influence the accuracy of parameterized equivalent circuit models. In certain cases, the optimal parameter set yields up to 82% lower RMSE than the error value averaged across all the parameter sets obtained. Consequently, the simplest first-order Thevenin model based on optimal parameterization protocol can be more accurate than the second-order ECM parameterized using an arbitrarily chosen test pulse. It was concluded that the moderate test pulse amplitude (0.5 C) is preferable, as the higher current values intensify the non-linear portion of the cell voltage response, which can not be described by the considered ECM. The optimal combination of the test pulse duration and the relaxation data cut-off depends on the particular validation profile, i.e., battery operation regime. However, if a thorough optimization of the parameter identification protocol is out of the question due to practical limitations, we suggest that setting both the pulse duration and the relaxation data cutoff to about 2 minutes should be a good 'blind guise' according to most of our

validation tests. Finally, by selecting the optimal parameter set, we were able to reach remarkably low model error (RMSE = 1.2 mV) for a current profile close to a real-life electric vehicle battery operation regime.

Author Contributions: Conceptualization, A.S.; Investigation, D.G., A.S.; Formal analysis, A.S., A.D, D.G.; Visualization, A.D; Writing - original draft, A.S., A.D, D.G. All authors have read and agreed to the published version of the manuscript.

Funding: This work was funded by the Ministry of Science and Higher Education of the Russian Federation (Goszadanie) 0075-03-2025-662, project No. FSMG-2024-0046.

Data Availability Statement: The obtained experimental data are available at zenodo.org: <https://zenodo.org/records/17635365> (DOI 10.5281/zenodo.17635365).

Conflicts of Interest: The authors declare no conflicts of interest.

Abbreviations

The following abbreviations are used in this manuscript:

BMS	Battery Management System
ECM	Equivalent Circuit Model
RMSE	Root Mean Square Error
SoC	State of Charge
SoH	State of Health
OCV	Open Circuit Voltage

References

1. Plett, G.L. Battery Management Systems, Volume I: Battery Modeling; Artech House, 2015;
2. Doyle, M.; Fuller, T.F.; Newman, J. Modeling of Galvanostatic Charge and Discharge of the Lithium/Polymer/Insertion Cell. *J Electrochem Soc* **1993**, *140*, 1526–1533. <https://doi.org/10.1149/1.2221597>.
3. Newman, J.; Thomas-Alyea, K.E. *Electrochemical Systems*; 3rd ed.; John Wiley & Sons: New Jersey, 2012; ISBN 978-0-471-47756-3.
4. Ramadesigan, V.; Northrop, P.W.C.; De, S.; Santhanagopalan, S.; Braatz, R.D.; Subramanian, V.R. Modeling and Simulation of Lithium-Ion Batteries from a Systems Engineering Perspective. *J Electrochem Soc* **2012**, *159*, R31–R45. <https://doi.org/10.1149/2.018203jes>.
5. Severson, K.A.; Attia, P.M.; Jin, N.; Perkins, N.; Jiang, B.; Yang, Z.; Chen, M.H.; Aykol, M.; Herring, P.K.; Fragedakis, D.; et al. Data-Driven Prediction of Battery Cycle Life before Capacity Degradation. *Nat Energy* **2019**, *4*, 383–391. <https://doi.org/10.1038/s41560-019-0356-8>.
6. Ren, Z.; Du, C. A Review of Machine Learning State-of-Charge and State-of-Health Estimation Algorithms for Lithium-Ion Batteries. *Energy Reports* **2023**, *9*, 2993–3021. <https://doi.org/10.1016/j.egy.2023.01.108>.
7. He, H.; Xiong, R.; Guo, H.; Li, S. Comparison Study on the Battery Models Used for the Energy Management of Batteries in Electric Vehicles. *Energy Convers Manag* **2012**, *64*, 113–121. <https://doi.org/10.1016/j.enconman.2012.04.014>.
8. Jossen, A. Fundamentals of Battery Dynamics. *J Power Sources* **2006**, *154*, 530–538. <https://doi.org/10.1016/j.jpowsour.2005.10.041>.
9. Li, J.; Klee Barillas, J.; Guenther, C.; Danzer, M.A. A Comparative Study of State of Charge Estimation Algorithms for LiFePO₄ Batteries Used in Electric Vehicles. *J Power Sources* **2013**, *230*, 244–250. <https://doi.org/10.1016/j.jpowsour.2012.12.057>.
10. Stroe, A.I.; Stroe, D.I.; Swierczynski, M.; Teodorescu, R.; Kær, S.K. Lithium-Ion Battery Dynamic Model for Wide Range of Operating Conditions. *Proceedings - 2017 International Conference on Optimization of*

- Electrical and Electronic Equipment, OPTIM 2017 and 2017 Intl Aegean Conference on Electrical Machines and Power Electronics, ACEMP 2017 **2017**, 660–666. <https://doi.org/10.1109/OPTIM.2017.7975044>.
11. Saldaña, G.; San Martín, J.I.; Zamora, I.; Asensio, F.J.; Oñederra, O. Analysis of the Current Electric Battery Models for Electric Vehicle Simulation. *Energies (Basel)* **2019**, *12*, 2750. <https://doi.org/10.3390/en12142750>.
 12. Bruch, M.; Millet, L.; Kowal, J.; Vetter, M. Novel Method for the Parameterization of a Reliable Equivalent Circuit Model for the Precise Simulation of a Battery Cell's Electric Behavior. *J Power Sources* **2021**, 490. <https://doi.org/10.1016/j.jpowsour.2021.229513>.
 13. Plett, G.L. Extended Kalman Filtering for Battery Management Systems of LiPB-Based HEV Battery Packs - Part 3. State and Parameter Estimation. *J Power Sources* **2004**, *134*, 277–292. <https://doi.org/10.1016/j.jpowsour.2004.02.033>.
 14. Jeffrey R. Belt Battery Test Manual For Plug-In Hybrid Electric Vehicles; 2010;
 15. LeBel, F.A.; Messier, P.; Sari, A.; Trovão, J.P.F. Lithium-Ion Cell Equivalent Circuit Model Identification by Galvanostatic Intermittent Titration Technique. *J Energy Storage* **2022**, *54*. <https://doi.org/10.1016/j.est.2022.105303>.
 16. Hu, Y.; Wang, Y.Y. Two Time-Scaled Battery Model Identification with Application to Battery State Estimation. *IEEE Transactions on Control Systems Technology* **2015**, *23*, 1180–1188. <https://doi.org/10.1109/TCST.2014.2358846>.
 17. Zhang, R.; Xia, B.; Li, B.; Lai, Y.; Zheng, W.; Wang, H.; Wang, W.; Wang, M. Study on the Characteristics of a High Capacity Nickel Manganese Cobalt Oxide (NMC) Lithium-Ion Battery-an Experimental Investigation. *Energies (Basel)* **2018**, *11*. <https://doi.org/10.3390/en11092275>.
 18. Cao, W.; Wang, S.; Fernandez, C.; Zou, C.; Yu, C.; Li, X. A Novel Adaptive State of Charge Estimation Method of Full Life Cycling Lithium-ion Batteries Based on the Multiple Parameter Optimization. *Energy Sci Eng* **2019**, *7*, 1544–1556. <https://doi.org/10.1002/ese3.362>.
 19. Zhang, H.; Deng, C.; Zong, Y.; Zuo, Q.; Guo, H.; Song, S.; Jiang, L. Effect of Sample Interval on the Parameter Identification Results of RC Equivalent Circuit Models of Li-Ion Battery: An Investigation Based on HPPC Test Data. *Batteries* **2022**, *9*, 1. <https://doi.org/10.3390/batteries9010001>.
 20. Stroe, D.-I.; Swierczynski, M.; Stroe, A.-I.; Knudsen Kær, S. Generalized Characterization Methodology for Performance Modelling of Lithium-Ion Batteries. *Batteries* **2016**, *2*, 37. <https://doi.org/10.3390/batteries2040037>.
 21. Saleem, K.; Mehran, K.; Ali, Z. Online Reduced Complexity Parameter Estimation Technique for Equivalent Circuit Model of Lithium-Ion Battery. *Electric Power Systems Research* **2020**, *185*, 106356. <https://doi.org/10.1016/j.epsr.2020.106356>.
 22. Zheng, Y.; Gao, W.; Han, X.; Ouyang, M.; Lu, L.; Guo, D. An Accurate Parameters Extraction Method for a Novel On-Board Battery Model Considering Electrochemical Properties. *J Energy Storage* **2019**, *24*, 100745. <https://doi.org/10.1016/j.est.2019.04.019>.
 23. Hentunen, A.; Lehmuspelto, T.; Suomela, J. Time-Domain Parameter Extraction Method for Thévenin-Equivalent Circuit Battery Models. *IEEE Transactions on Energy Conversion* **2014**, *29*, 558–566. <https://doi.org/10.1109/TEC.2014.2318205>.
 24. Cittanti, D.; Ferraris, A.; Airale, A.; Fiorot, S.; Scavuzzo, S.; Carello, M. Modeling Li-Ion Batteries for Automotive Application: A Trade-off between Accuracy and Complexity. In *Proceedings of the 2017 International Conference of Electrical and Electronic Technologies for Automotive; IEEE, June 2017; pp. 1–8*.
 25. Campagna, N.; Castiglia, V.; Miceli, R.; Mastromauro, R.A.; Spataro, C.; Trapanese, M.; Viola, F. Battery Models for Battery Powered Applications: A Comparative Study. *Energies (Basel)* **2020**, *13*, 4085. <https://doi.org/10.3390/en13164085>.
 26. Ceraolo, M.; Lutzemberger, G.; Poli, D.; Scarpelli, C. Model Parameters Evaluation for NMC Cells. In *Proceedings of the 2019 IEEE International Conference on Environment and Electrical Engineering and 2019 IEEE Industrial and Commercial Power Systems Europe (EEEIC / I&CPS Europe); IEEE, June 2019; pp. 1–6*.

27. Dvorak, D.; Bauml, T.; Holzinger, A.; Popp, H. A Comprehensive Algorithm for Estimating Lithium-Ion Battery Parameters From Measurements. *IEEE Trans Sustain Energy* **2018**, *9*, 771–779. <https://doi.org/10.1109/TSTE.2017.2761406>.
28. Li, Z.; Shi, X.; Shi, M.; Wei, C.; Di, F.; Sun, H. Investigation on the Impact of the HPPC Profile on the Battery ECM Parameters' Offline Identification. In Proceedings of the 2020 Asia Energy and Electrical Engineering Symposium (AEEES); IEEE, May 2020; pp. 753–757.
29. Dynamometer Drive Schedules Available online: <https://www.epa.gov/vehicle-and-fuel-emissions-testing/dynamometer-drive-schedules> (accessed on 27 September 2025).
30. Mesbahi, T.; Khenfri, F.; Rizoug, N.; Chaaban, K.; Bartholomeüs, P.; Le Moigne, P. Dynamical Modeling of Li-Ion Batteries for Electric Vehicle Applications Based on Hybrid Particle Swarm–Nelder–Mead (PSO–NM) Optimization Algorithm. *Electric Power Systems Research* **2016**, *131*, 195–204. <https://doi.org/10.1016/j.epsr.2015.10.018>.
31. Micari, S.; Foti, S.; Testa, A.; De Caro, S.; Sergi, F.; Andaloro, L.; Aloisio, D.; Leonardi, S.G.; Napoli, G. Effect of WLTP CLASS 3B Driving Cycle on Lithium-Ion Battery for Electric Vehicles. *Energies (Basel)* **2022**, *15*, 6703. <https://doi.org/10.3390/en15186703>.
32. Charbonneau, V.; Lasia, A.; Brisard, G. Impedance Studies of Li⁺ Diffusion in Nickel Manganese Cobalt Oxide (NMC) during Charge/Discharge Cycles. *Journal of Electroanalytical Chemistry* **2020**, 875. <https://doi.org/10.1016/j.jelechem.2020.113944>.

Disclaimer/Publisher's Note: The statements, opinions and data contained in all publications are solely those of the individual author(s) and contributor(s) and not of MDPI and/or the editor(s). MDPI and/or the editor(s) disclaim responsibility for any injury to people or property resulting from any ideas, methods, instructions or products referred to in the content.